RESEARCH ARTICLE

Diversity and dynamics of Antarctic marine microbial eukaryotes under manipulated environmental UV radiation

Anouk M.-T. Piquet[1,2], Henk Bolhuis[3], Andrew T. Davidson[4], Paul G. Thomson[4] & Anita G.J. Buma[1]

[1]Department of Ocean Ecosystems, Centre for Ecological and Evolutionary Studies, University of Groningen, Haren, The Netherlands; [2]Department of Microbial Ecology, Centre for Ecological and Evolutionary Studies, University of Groningen, Haren, The Netherlands; [3]Department of Marine Microbiology, NIOO-KNAW, Yerseke, The Netherlands; and [4]Australian Antarctic Division and Antarctic Climate and Ecosystems Cooperative Research Centre, Kingston, Tasmania, Australia

Correspondence: Anouk M.-T. Piquet, Department of Ocean Ecosystems, Biological Centre, PO Box 14, 9750 AA Haren, The Netherlands. Tel.: +31 50 363 2286; fax: +31 50 363 2261; e-mail: a.m.t.piquet@rug.nl

Received 6 August 2007; revised 25 June 2008; accepted 30 July 2008.
First published online 17 September 2008.

DOI:10.1111/j.1574-6941.2008.00588.x

Editor: Riks Laanbroek

Keywords
Antarctic; marine micro-eukaryotes; 18S rRNA gene; DGGE; diversity; UV radiation.

Abstract

In the light of the predicted global climate change, it is essential that the status and diversity of polar microbial communities is described and understood. In the present study, molecular tools were used to investigate the marine eukaryotic communities of Prydz Bay, Eastern Antarctica, from November 2002 to January 2003. Additionally, we conducted four series of minicosm experiments, where natural Prydz Bay communities were incubated under six different irradiation regimes, in order to investigate the effects of natural UV radiation on marine microbial eukaryotes. Denaturing gradient gel electrophoresis (DGGE) and 18S rRNA gene sequencing revealed a eukaryotic Shannon diversity index averaging 2.26 and 2.12, respectively. Phylogenetic analysis of 472 sequenced clones revealed 47 phylotypes, belonging to the *Dinophyceae*, Stramenopiles, Choanoflagellidae, *Ciliophora*, *Cercozoa* and Metazoa. Throughout the studied period, three communities were distinguished: a postwinter/early spring community comprising dinoflagellates, ciliates, cercozoans, stramenopiles, viridiplantae, haptophytes and metazoans; a dinoflagellate-dominated community; and a diatom-dominated community that developed after sea ice breakup. DGGE analysis showed that size fraction and time had a strong shaping effect on the community composition; however, a significant contribution of natural UV irradiance towards microeukaryotic community composition could not be detected. Overall, dinoflagellates dominated our samples and their diversity suggests that they fulfill an important role in Antarctic coastal marine ecosystems preceding ice breakup as well as between phytoplankton bloom events.

Introduction

Marine phytoplankton plays a central role in the global carbon cycle, accounting for half of the global primary production (Falkowski *et al.*, 1998). It has been estimated that in the Southern Ocean, photosynthesis by phytoplankton is responsible for up to 15% of global marine primary production (Huntley *et al.*, 1991). Through grazing on primary producers, organic carbon is transferred to higher trophic levels (El-Sayed, 1993; Le Fèvre *et al.*, 1998). Additionally, a variable fraction of the organic carbon eventually sediments to the ocean floor in the form of particulate organic carbon (POC), which consists of aggregates of decayed cell material or fecal pellets. This enables significant quantities of anthropogenically emitted CO_2 to be fixed and stored in the deep ocean (Arrigo *et al.*, 1999; Raven & Falkowski, 1999), a process known as the biological pump (Karl, 1993).

The observed increases in atmospheric CO_2 led to numerous studies from different scientific disciplines devoted to climate change. Specifically, trends in temperature increase, enhanced ice-melting rates, glacial shelf calving and increased wind speeds are measured (Shepherd & Wingham, 2007). Most studies demonstrate that climate change is occurring faster than expected, especially in the polar regions, including the Antarctic. Another feature

related to climate change is the yearly recurring spring time stratospheric ozone depletion that enhances surface-incident biologically effective UV-B (280–315 nm) radiation. *In situ* and experimental measurements on the effects of UV-B radiation on marine organisms have reported effects on species composition (Villafañe *et al.*, 1995; Mousseau *et al.*, 2000; Davidson & Belbin, 2002; Wängberg & Wulff, 2004) as well as significant decreases in production rates, both affecting total carbon flow and fixation rate (Holm-Hansen *et al.*, 1993; Arrigo *et al.*, 2003).

Predicting and understanding future shifts induced by climate change requires a thorough description of the present status, diversity and dynamics of marine eukaryote communities. Application of molecular techniques in the study of eukaryote community structure offers an increased resolution compared with the classical approaches. For example, classical identification procedures (light microscopy and scanning electron microscopy) may not always be appropriate for microeukaryotes, especially the flagellates including the nanoflagellate phytoplankton classes that are abundantly present in Antarctic waters (Weber & El-Sayed, 1987). Flagellates are extremely difficult to identify by microscopy due to their fragility and cryptic morphologic (Gast *et al.*, 2004), while other well-established approaches such as pigment fingerprinting methods provide information on the class level only (DiTullio *et al.*, 2003). As a result, molecular tools may add valuable new insights to Antarctic eukaryotic diversity. So far, molecular studies on the diversity of marine microbial eukaryotes constitute a fraction of the large number of studies devoted to prokaryotic diversity. The discrepancy between prokaryote- and eukaryote-based culture-independent studies is even greater when only polar regions are considered. For Eastern Antarctic coastal waters, information on the diversity of marine microbial eukaryotes is limited and restricted to taxonomic characterization using microscopy.

In this study, we conducted a molecular analysis on the microeukaryotic ($< 200\,\mu m$) diversity of Prydz Bay, Antarctica, at Davis station, from spring to summer 2002–2003. A combination of partial 18S rRNA gene sequencing and eukaryotic fingerprinting carried out using denaturing gradient gel electrophoresis (DGGE) was applied. A series of experiments was conducted with these natural communities and was repeated four times from October to January. Natural assemblages were incubated for 2 weeks under six different natural UV-radiation (280–400 nm, UV-R) conditions varying from visible light only (400–700 nm) to the full solar spectrum including UV-R. Shifts in the natural marine protistan assemblage were followed after 7 and 14 days of incubation using DGGE analysis. We hypothesize that different UV-irradiances cause shifts in the eukaryote community, due to known differences in species-specific sensitivity to UV-R (Karentz *et al.*, 1991; Davidson *et al.*, 1994).

Materials and methods

Experimental set up

Four experiments were conducted at Davis Station, Australian Antarctic Division, (68°35′S, 77°58′E) between November 2002 and January 2003. Coastal Antarctic seawater was pumped from 60 m offshore (*c.* 2 m depth) directly into minicosm tanks using food-grade plumbing and a Teflon diaphragm pump to minimize both contamination of the seawater and physical damage to the microbial community. The intake was covered with a 200-μm mesh to exclude mesozooplankton. Samples for experiments 1–3 were obtained through a hole drilled in the sea ice. Samples for experiment 4 were collected later in summer, when the sea ice had disappeared. Accordingly, a buoy and anchor were deployed to pump water from the same location and depth as the first three series.

Incubations were performed in 6×650-L minicosm tanks (150 cm high, 80 cm diameter) constructed of natural polyethylene that were housed in a refrigerated shipping container. The minicosm tanks were filled simultaneously to ensure an identical starting community and then incubated for 14 days, except for experiment 3 (13 days), at ambient temperature $\pm \leq 0.84\,^{\circ}C$. Each minicosm was gently mixed by a paddle set at 3 r.p.m. to prevent cell sedimentation and ensure vertical mixing of the community over the entire water column. The minicosms were maintained at a constant temperature by the refrigeration of the shipping container. Following 0, 7 and 14 days of incubation (T_0, T_7 and T_{14}, respectively) 2-L samples of the microbial community from each minicosm tank were obtained via Teflon sample lines fitted to the tank (100 cm height).

Solar radiation was channeled into the minicosms by a reflector tube placed between the tank and the UV-R transmissive acrylic dome located on the roof of the shipping container. Attenuating screens placed directly above the minicosm tanks were used to spectrally differentiate UV-R entering each minicosm; this resulted in six distinct irradiance treatments (Fig. 1). The UV-R cut-off screens had relative transmittances ranging from 1.00 (Acrylic) to 0.04 (Polycarbonate), corresponding to irradiance regimes experienced by organisms at 4.4 and 12.2 m depth, respectively (Table 1).

Daily solar radiation was measured throughout each 14-day experiment using instruments mounted on the roof of the shipping container: a LI-COR LI-190SA Quantum sensor measured photosynthetically active radiation (PAR, 400–700 nm) and a Solar Light Company 501A UV Biodosimeter measured erythemally weighted UV-R (Ultra-Violet Radiation, 280–400 nm). The average irradiance transmitted into the water column over total depth was calculated both considering attenuation by water and by biomass [Eqn. (1)].

$$\bar{I} = \frac{I_0}{kd}(1 - e^{-kd}). \quad (1)$$

The cumulative erythemal doses received in each tank were calculated from the down-welling irradiance data by taking into account the attenuation by the dome, reflective tube, attenuator screens and the water column. Average irradiation transmitted into the water column was calculated over the total depth, where I_0 is the incoming irradiance before it passes through the water column, k: the attenuation coefficient (sum of k_{water} and $k_{biomass}$) and d the total water column depth using Beer's law (transmittance $T = e^{-kd}$).

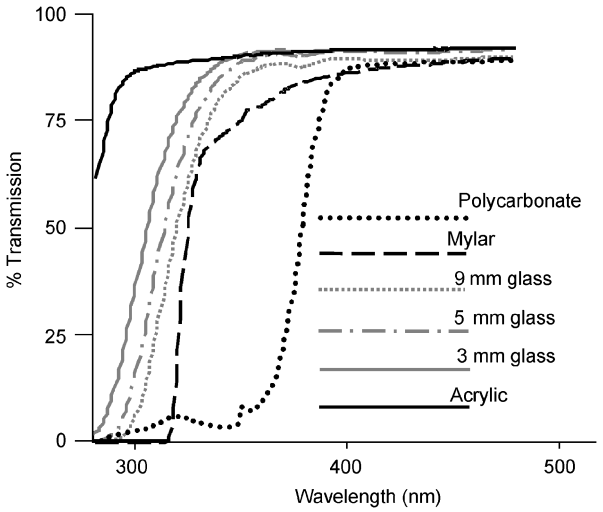

Fig. 1. Spectral transmission characteristics of the filter materials used for the experiments. Polycarbonate-covered minicosm 1; mylar, minicosm 2; glass of 9, 5 and 3 mm thickness, minicosms 3–5 respectively; and acrylic, minicosm 6.

Sample handling

Since earlier studies had demonstrated high relative UV-R vulnerability for the smallest phytoplankton size fractions (Villafañe *et al.*, 1995; Buma *et al.*, 2001), samples were fractionated into distinct size fractions to discriminate possible size-related differences in UV-R effects. Two-liter samples were successively filter fractionated onto 10- and 2-μm pore-size polycarbonate filters (Millipore), giving two fraction sizes: 200-10 μm (henceforth referred to as the 10 μm fraction), which would contain larger phytoplankton cells such as diatoms, and 10–2 μm (henceforth the 2 μm fraction), which would mainly contain smaller phytoplankton cells such as phytoflagellates and nanoplanktonic diatoms. The samples were stored in 1.5 mL sterile lysis buffer (EDTA 40 mmol L^{-1}; Tris-HCl 50 mmol L^{-1}, pH 8.5; sucrose 0.75 mol L^{-1}) at −80 °C until further processing.

Nucleic acid extraction

All filter-handling steps were performed under sterile conditions. The filters were first cut into small pieces; then, to insure complete disruption of cells, each sample was

Table 1. Cumulative downwelling erythemal UV-R dose (J m^{-2}) for each minicosm tank

		Minicosm 1	Minicosm 2	Minicosm 3	Minicosm 4	Minicosm 5	Minicosm 6
Screen		Polycarbonate	Mylar	9-mm glass	5-mm glass	3-mm glass	Acrylic
Relative transmittance		0.04	0.14	0.34	0.68	0.81	1.00
Depth equivalent (m)		12.24	9.43	7.15	5.38	4.97	4.43
Irradiance regime		PAR	P+UVA	P+A+UVB1	P+A+UVB2	P+A+UVB3	P+A+UVB4
Treatment code		P	A	B1	B2	B3	B4
	Time	Cumulated erythemal dose					
Experiment 1	0	0.08	0.23	0.58	1.18	1.39	1.72
	7	39.87	122.58	305.3	620.25	729.29	906.22
	14	81.96	253.42	629.45	1278.93	1472.99	1861.31
Experiment 2	0	0.13	0.23	1.01	2.06	2.42	3.01
	7	38.74	122.58	269.69	602.96	707.93	877.95
	14	82.57	253.42	632.98	1299.45	1492.97	1863.99
Experiment 3	0	0.11	0.35	0.86	1.75	2.06	2.56
	7	51.42	158.55	394.8	797.08	938.04	1163.06
	13	88.94	274.3	678.19	1379.64	1628.41	2003.26
Experiment 4	0	0.11	0.35	0.84	1.17	2.01	2.49
	7	40.77	158.55	318.6	657.68	724.21	936.05
	14	78.80	274.3	617.14	1312.38	1394.56	1840.88

Cumulative erythemal dose measured after 0, 7 and 14 days incubation. Experimental details are given for the distinctive irradiation regimes applied for each minicosm: the attenuator screen material, its relative transmittance and depth equivalent, the created irradiance regime and corresponding treatment codes.

preheated at 70 °C for 5 min and bead beaten at maximum speed (Mini-Beadbeater™, Biospec Products) for 1 min with 0.1-mm diameter zirconia/silica beads (Biospec Inc.). To maximize DNA recovery from cell material, samples were incubated for 30 min at 37 °C with lysozyme (1 mg mL^{-1}) and for 30 min at 50 °C with 1% sodium dodecyl sulfate (SDS) and 0.1 mg mL^{-1} proteinaseK. DNA was subsequently extracted using a classical chloroform–phenol extraction, followed by standard sodium acetate and ethanol precipitation and washing steps (Sambrook *et al.*, 1989). The DNA pellet was resuspended in a sterile MilliQ and purified using the Wizard DNA Clean-Up kit (Promega).

PCR amplification

The samples were amplified using eukaryote-specific primers Euk1A (5′-CTGGTTGATCCTGCCAG-3′) and 516R (5′-ACCAGACTTGCCCTCC-3′) for partial amplification of the 18S rRNA gene (Díez *et al.*, 2001). The reverse primer was extended at the 5′ end with a GC-rich clamp for further use of the amplicons in denaturing gradient gel electrophoresis (DGGE) analysis (Díez *et al.*, 2001; Muyzer *et al.*, 2004). Fifty microliters of PCR mixtures consisted of dNTP mix in a final concentration of 200 μmol L^{-1}, primers (300 nmol L^{-1}), PCR buffer (1 ×, Amersham), $MgCl_2$ (3.25 mmol L^{-1}), formamide (1%), bovine serum albumin (0.2 mg mL^{-1}, Roche) and Taq DNA polymerase (2.5 U, Amersham). The reaction was run on a thermal cycler (GeneAmp®, PCR system 9700, Applied Biosystem) using the following program: 94 °C for 130 s; 35 cycles of 94 °C for 30 s, 56 °C for 45 s, 72 °C for 130 s and finally 72 °C for 7 min (Díez *et al.*, 2001). PCR products were separated using DNA gel electrophoresis on a 1% agarose gel, stained with ethidium bromide and visualized with an Image Master (Pharma Biotech). Amplicon yield was estimated by comparing bands with a DNA Smart Ladder (Eurogentec).

DGGE

DGGE was run on the PhorU system (Ingeny, Goes, the Netherlands) as described previously (Muyzer *et al.*, 2004). The best separation was obtained with a 20–55% urea–formamide 6% acrylamide (37.5 : 1, Biorad) denaturing gradient with 100% urea–formamide being defined as 7 mol L^{-1} Urea (Biorad) and 40% deionized Formamide (Sigma). Two hundred nanograms of the PCR product was loaded with loading buffer (0.05% w/v bromophenol blue, 40% sucrose, 0.1 mol L^{-1} EDTA pH 8.0, 0.5% sodium lauryl sulfate) for each sample. A reference sample was added as a normalization marker for subsequent cluster analysis. The samples were run for 16 h at 100 V in 0.5 × TAE buffer and subsequently stained with Sybr®GOLD (Molecular Probes) and visualized with UV-R using the Image Master (Pharma Biotech).

DGGE pattern analysis

The DGGE patterns were analyzed using BIONUMERICS® version 3.5 (Applied Biomaths). The gels were digitized and normalized using the flanking marker bands. Automated band calling was performed using BIONUMERICS with the standard detection settings (the manufacturer's protocol). However, a few flaws were detected: stains in the gel lead to false-positives and bands with low intensity remained undetected. Consequently, a visual check of the band patterns obtained was performed in order to remove false-positives and add low-intensity bands. The DGGE patterns for each sample were entered in the database and further analyzed by comparing the band patterns. Cluster analyses based on the presence of shared bands were performed with Dice similarity (as provided by the BIONUMERICS software). Results were presented in the form of an unweighted pair group method using an arithmetic averages (UPGMA) dendrogram.

Data analysis

The relationships between community structure (presence and absence data) and the variables: time, fraction size and UV-R were explored using gradient analysis (CANOCO 4.5). The data set was first analyzed using a detrended correspondence analysis (DCA) (ter Braak & Šmilauer, 1998) to explore the gradient length of the data set. Redundancy analysis (RDA) was applied for gradient lengths < 2; statistical significance of the generated ordination axes was tested for each analysis using Monte Carlo permutation tests. RDA was first performed with all environmental variables (time, fraction size and UV-R). Subsequently, each variable was tested separately to determine their individual structuring influence on the community.

Clone libraries and sequencing

For the construction of a clone library, we chose the (Euk1A-516) PCR primer combination rather than the commonly used EukA and EukB primer set that amplifies almost the complete 18S rRNA gene (Medlin *et al.*, 1988). Although sequencing the entire 18S rRNA gene fragment would have provided more phylogenetic information on the sequenced clone, we chose the Euk1A-516 set in order to match the region targeted using DGGE. PCR amplicons used for the DGGE analysis were also used to generate clone libraries for the 10 μm samples taken at T_0 and T_{14} (PAR treatment). Based on the DGGE band patterns generated sequencing efforts were limited to the 10-μm fraction size. The amplicons were cloned using the pGEM-T easy vector system (Promega) and transformed into *Escherichia coli* JM109-competent cells. Positive inserts were amplified using the SP6 and T7 primers that have their target sites located on the vector. Amplicons were sequenced on an ABI PRISM® 377

sequencer using the T7 primer. Sequences of 700 bp, including the entire insert, were manually checked with CHROMAS 2.3 (Technelysium, Australia). Additionally, poor-quality and suspected chimeras were checked using th eBLAST and the CHIMERA CHECK program from the Ribosomal Data Project (Michigan State University, http://rdp8.cme.msu.edu/cgis/chimera.cgi?su=SSU). Multiple sequence alignments using CLUSTALW and phylogenetic and molecular evolutionary analyses were performed using the MEGA version 3.1 and 4.0 (Kumar *et al.*, 2004; Tamura *et al.*, 2007). Sequences were assigned to major groups by comparison with the BLAST sequences of the GenBank database (National Center for Biotechnology Information, http://www.ncbi.nlm.nih.gov), which were also included in the alignment and phylogenetic analysis. Phylogenetic trees were constructed in MEGA 4.0 by the neighbor-joining (Saitou & Nei, 1987) analysis of aligned sequences using the maximum composite likelihood algorithm (Hartl *et al.*, 1994; Zhu & Bustamante, 2005) and 1000 bootstrap repeats (Felsenstein, 1985). For comparison, we also ran the neighbor-joining analysis using the Kimura-2-parameter model (Kimura, 1980) but this did not result in large differences in tree topology. Operational taxonomic units (OTU) are defined as sequences with at least 97% identity. Clone sequences that showed 93% or less identity with a cultivated or an environmental clone sequence were defined as novel sequences. Clones with more than 93% identity to only environmental clone sequences were classified as uncultivated OTUs.

DGGE band identification

Initially, direct band excision and subsequent reamplification was performed; however, reamplified products proved to regenerate the entire environmental band pattern. The process of excision, reamplification and DGGE comparison had to be repeated at least five times until it yielded a single band. This approach only provided sequences for a few bands from experiment 2, which were included in the analysis. Because direct band sequencing was not feasible within reasonable time span, clone libraries generated for sequencing purposes were run on the DGGE next to the corresponding environmental sample. Similarities in migration patterns between the clones and band patterns were used to select clones for sequencing. Bands were only positively identified if at least two clones with similar migration positions yielded similar sequences. The generated sequences were included in the phylogenetic analysis.

Diversity analysis

Clone sequences were classified into OTUs according to a 97% sequence similarity cut-off level and used subsequently in the diversity analysis. The Shannon–Wiener diversity index of sequence data was calculated from the relative abundance of sequences per defined OTU. Diversity indexes were also calculated for the DGGE patterns. The total number of bands and their respective relative abundance were determined using the BIONUMERICS and used to calculate the sample diversity. All the diversity indexes were calculated using PAST (PALaeontological Statistics analysis program, http://folk.uio.no/ohammer/past/).

Nucleotide sequence accession numbers

One sequence for each OTU (47 in total) reported in this study has been deposited in GenBank under accession numbers EU078274–EU078320.

Results

Cumulative erythemal UV dose

The average daily erythemal dose measured at Davis station (68°35′S) from November 2002 to January 2003 was 2.5, 2.7, 3.2 and 3.2 kJ m^{-2} during experiments 1, 2, 3 and 4, respectively. As a comparison, for the same periods from November 2000 to January 2006, Palmer station (64°46′S) average daily erythemal dose ranged from 2.6 to 3.5 kJ m^{-2} and 2.7 to 4.0 kJ m^{-2} for McMurdo Station (77°50′S) (http://www.biospherical.com/nsf). Overall, daily erythemal doses measured at Davis matched the irradiance values expected for an Antarctic location.

During the experiments, incident irradiance and its derived cumulative erythemal UV-R doses increased approximately linearly over the incubation period. Although the spectral transmittance of the UV-R cut-off screens (Fig. 1) suggested little differences between treatments, the UV-R erythemal dose experienced by the communities in the different minicosms differed strongly between UV-R treatments (Table 1). For example, after 14 days of incubation the communities in minicosm 3 (9-mm glass) and minicosm 4 (5-mm glass) had experienced an average cumulative erythemal dose of 639.5 and 1317.7 J m^{-2}, respectively. The erythemal dose measured for each UV-treatment was highly similar between experiments (Table 1). After 14 days of incubation, the UV-R erythemal dose experienced by the communities ranged from the lowest dose averaging 83.1 J m^{-2} in the 'PAR treatment' to the highest dose of 1892.5 J m^{-2} in the 'all UV-R treatment'.

Dynamics of the eukaryotic communities incubated under variable UV-R

DGGE band patterns were generated for all samples that yielded PCR products. A few samples failed to be amplified: 2-14-6-10,-2 [samples exposed to highest UV-irradiance (tank 6) at T_{14} from experiment 2] and 4-14-4-2, while

samples 3-7-3-10,-2 could not be sampled due to water shortage. DGGE band patterns obtained for experiments 1, 2, 3 and 4 (Fig. 2) were clustered according to Dice similarities; the data are presented in the form of a dendrogram on the left of each gel image. Our data reveal that DGGE banding patterns obtained for communities incubated under distinct UV irradiation conditions mainly clustered according to size fraction and incubation time. The different irradiance regimes did not induce major or consequent variation in community composition between the different minicosms (Fig. 2). Only a few sporadic effects of UV-R could be detected. In experiment 1, the 10 and 2 μm size fractions of sample 6 at T_{14} are the most divergent patterns in the dendrogram branching off at the edges of the dendrogram. After 7 days of incubation in the second experiment, samples 4, 5 and 6 (10 μm) cluster separately from communities exposed to the lower irradiance regimes (samples 1 and 2, 10 μm). Samples 4, 5 and 6 (10 μm) from experiment 3 incubated for 14 days cluster together away from the samples exposed to lower irradiance regimes (1, 2

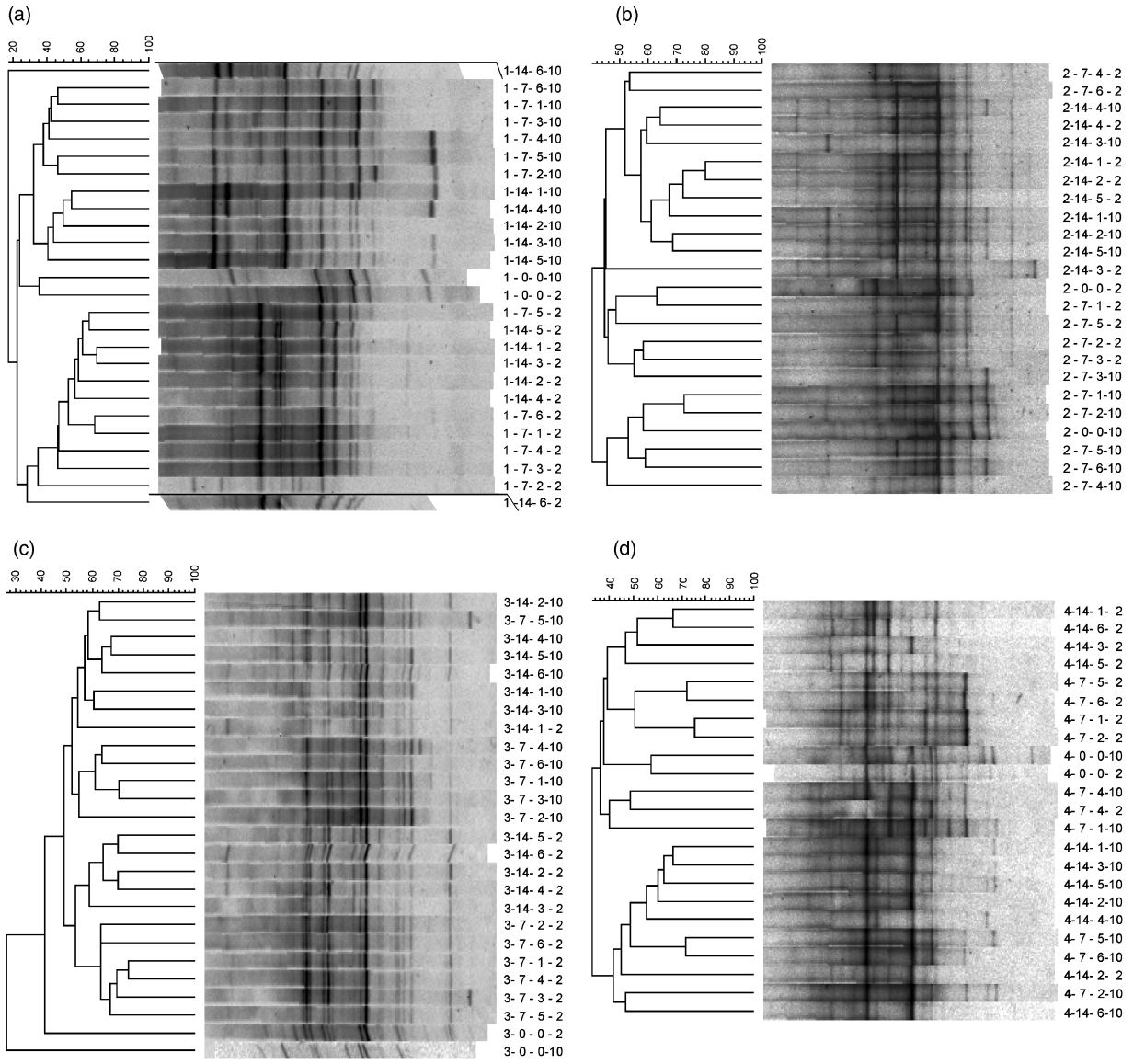

Fig. 2. DGGE band patterns obtained for all samples from each incubation experiment and corresponding UPGMA dendrograms obtained with Dice similarity analysis (a–d, experiments 1–4). Experiments are shown in a box each; sample numbers are indicated on the right hand side. Sample coding stands for: experiment number – sampling time – minicosm number – size fraction. For example, the first sample 1-0-0-10 is from experiment 1, collected at T_0, 0 stands for inoculum, size fraction 10 μm. The second sample 1-7-6-10 is from experiment 1, collected at T_7 from minicosm 6 and is size fraction 10 μm. Pearson's similarity scale is shown in percentages on the upper left hand side of each dendrogram.

and 3, 10 μm). At T_{14}, the 2-μm size fractions of samples 5 and 6 also form a separate cluster, however, showing strong similarities to samples 2 and 4. After 7 days of incubation both size fractions of samples 5 and 6 formed separate clusters in experiment 4. In order to determine whether the sporadic shifts observed for samples from tanks 4, 5 and 6 were caused by UV-R, variance in the presence–absence of bands was analyzed using ordination analysis.

DCA revealed that the lengths of gradients were < 2 in all experiments; we, therefore, used RDA to perform further ordination analysis of the data set. RDA analysis performed separately for each experiment explained 17.4%, 13.4%, 15.3% and 17.8% of the species variance (bands) in experiments 1, 2, 3 and 4, respectively. The environmental variables time, fraction size and UV-R together explained a significant part of the variation (Monte Carlo Permutation tests, $P < 0.001$). When the variables were tested separately only time ($P < 0.02$) and fraction size ($P < 0.001$) explained a significant part of the variation, while the environmental variable UV-R did not (experiments 1–4: $P = 0.442$; $P = 0.496$; $P = 0.110$; $P = 0.094$). We, therefore, conclude that in our experiments the DGGE band patterns generated for microeukaryotic communities were not structured by UV-R.

Community composition comparison

In order to compare the microeukaryotic communities of the four experiments, we ran both size fractions of the inoculum (T_0) and the T_{14} of communities exposed to PAR (henceforth $T_{14(P)}$) on a single DGGE (Fig. 3). Herewith, band patterns obtained for the different experiments became comparable. Phylogenetic analysis of the sequences corresponding to bands from different experiments but with similar migration pattern proved to cluster within the same OTU. We, therefore, conclude that in the present study, bands from different experiments with identical migration pattern represented the same species. Band identification by sequencing (Table 2) revealed a diverse community in experiment 1 including dinoflagellates, diatoms, haptophytes, viridiplantae and copepods. Most bands from experiments 2 and 3 represented fragments of partial 18S rRNA gene related to dinoflagellates (*Dinophyceae* sp., *Prorocentrum* sp. and *Gymnodinium* sp.); in experiment 4, bands were mostly related to diatom species (*Thalassiosira* sp., *Fragilaria* sp. and *Navicula* sp.) and cercozoan species.

The DGGE pattern obtained for the T_0 and $T_{14(P)}$ samples (Fig. 3a) revealed several DGGE bands that were present in more than one experiment and sometimes throughout all experiments. Cluster analysis of the DGGE patterns revealed a dendrogram showing three main clusters (Fig. 3b). The upper cluster (I) mainly contained the larger fraction of the T_0 samples of experiments 1, 2 and 3, which were all collected directly under the sea ice. From experiment 1, the

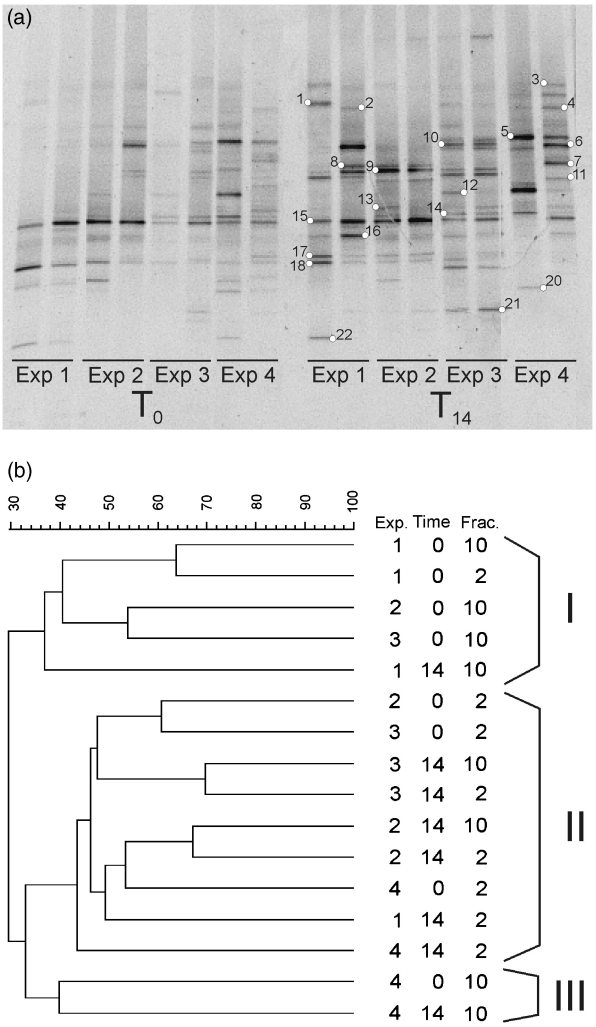

Fig. 3. DGGE and the corresponding cluster analysis obtained for the banding pattern of T_0 and $T_{14(P)}$ samples from all experiments. (a) Image of the DGGE gel. Experiment numbers and incubation time are indicated in the lower part of the gel; each sample is presented in pairs: 10 and 2 μm. Numbers shown within the gel correspond to the bands identified by sequencing (see Table 2 for band identity). (b) UPGMA dendrogram showing the clustering obtained with Dice similarity analysis of the band patterns. On the right hand side, the experiment number (Exp.), size fraction (Frac.) and incubation time (Time) are indicated. For clarity purposes the three major clusters described in the text are indicated by I, II and III. Similarity percentage between samples is indicated by the scale above the UPGMA tree.

$T_{14(P)}$ 10 μm sample was included in this cluster, indicating that after 14 days of incubation samples from experiment 1 remained very similar to the postwinter/early spring microbial eukaryotic community inhabiting the sub-ice water column. A large central cluster (cluster II, in Fig. 3b) included most 2-μm samples from all experiments as well as the 10-μm size fractions of $T_{14(P)}$ from experiments 2 and 3. Sequencing data collected for these samples indicated the

Table 2. Band identity as determined by sequence analysis, for the band numbers shown in Fig. 3a; the corresponding closest BLAST sequence, GenBank accession number and percentage similarity

Band	Class	OTU	BLAST	Accession no.	% identity
1	Str	E1-43	*Cylindrotheca closterium*	DQ082742	97
2	Str	E1-160	*Haslea crucigera*	AY485482	96
3	Choa	E3-143	*Diaphanoeca grandis*	AF084234	98
4	Cil	E1-21	*Tintinnopsis tocatinensis*	AY143561	96
5	Str	E4-130	*Fragilariopsis cylindrus*	EF140624	99
6	Str	E4-135	*Fragilaria* cf. *striatula*	AJ971377	99
7 and 11	Str	E4-155	*Navicula phyllepta*	AY485456	98
8 and 9	Viri	E2-153	*Pyramimonas aureus*	AB052289	98
10	Str	E4-55	*Pirsonia diadema*	AJ561114	91
12	Din	E4-160	*Thecadinium dragescoi*	AY238479	93
13	Din	E2-112	*Prorocentrum* sp.	AY803743	99
14 and 21	Din	E1-40	*Gymnodinium catenatum*	AY421785	98
15	Din	E1-166	*Dinophyceae* sp. *W5-1*	AY434687	99
16	Din	E2-55	*Gyrodinium spirale*	AB120001	99
16	Din	E3-56	*Protoperidinium pellucidum*	AB181903	93
17 and 18	Hapt	E1-140	*Phaeocystis pouchetii*	AF182114	99
20	Annel	E4-126	*Psamathe fusca*	DQ442595	99
22	Cope	E1-161	*Acanthocyclops viridis*	AY626999	95

Major taxonomic classes are coded by: Din, Dinoflagellates; Cil, Ciliates; Cerc, Cercozoa; Str, Stramenopiles; Choa, Choanoflagellates; Hapt, Haptophyceae; Viri, Viridiplantae; Annel, Annelidae; Cope, Copepoda.

strong dominance of dinoflagellates. Similarity analysis of the DGGE band patterns revealed a third cluster (III in Fig. 3b), which included the 10-μm size fractions of T_0 and $T_{14(P)}$ samples from experiment 4. These samples were taken after the sea ice had disappeared from Prydz Bay. Microscopy (data not shown), clone sequencing and subsequent band identification efforts indicated that the sample timing coincided with the onset of a diatom bloom. We, therefore, concluded that the lower cluster most likely resulted from this diatom-dominated community.

18S rRNA gene-based eukaryotic diversity

The composition of the eukaryotic community in each experiment was determined for each experiment using the 10 μm fraction of T_0 and $T_{14(P)}$. This generated a total of 472 clones. The number of clones sequenced per sample ranged between 51 and 66 clones. Sequence analysis yielded a total of 47 OTUs, defined as 18S rRNA gene sequences with $>$ 97% identity, which were divided over nine eukaryotic classes: *Dinophyceae*, Stramenopiles, *Cercozoa*, *Ciliophora*, Metazoa, Viridiplantae, *Haptophyceae*, *Choanoflagellidea* and *Ascomycota* (Fig. 4).

Out of the sequences analyzed, 64% were related to the Alveolates, which comprises the *Dinophyceae* and *Ciliophora*. Within the Dinophyceae three related OTUs grouped separately from any cultivated dinoflagellate sequence: i.e. the E4-160 OTU consisting of 25 clones, E3-56 consisting of nine clones and a single (nonchimeric) E1-34 clone. We propose that E4-160 and E1-34 are novel dinoflagellate OTUs, as all clones included within these OTUs had 93% or less sequence similarity to any cultivated eukaryote sequence or any environmental clone sequence. The E3-56 OTU represents a not yet cultivated dinoflagellate OTU (96% similarity to a eukaryote clone NA1 1C1). The most abundant dinoflagellate OTUs were related to *Gymnodinium catenatum* (E1-40, 81 clones), *Gyrodinium spirale* (E2-55, 75 clones), *Heterocapsa triquetra* (E3-121, 40 clones), *Pentapharsodinium tyrrhenicum* (E3-10, 27 clones) and *Dinophyceae* sp. (E1-166, 24 clones). Three OTUs (E4-46, E2-22 and E1-21) were related to the *Ciliophora*; E2-22 was related to a novel phylotype (93% similarity to any known sequence); and OTU E1-21 (three clones) was most related to the genus *Tintinnopsis* sp. Phylotype E4-46 was 96% similar to the *Strombodinium inclinatum*.

The second most dominant group of sequences belonged to the Stramenopiles, representing 16.3% of the clones. Centric diatoms were represented by sequences closely related to *Thalassiosira* sp., *Chaetoceros* sp., *Stellarima* sp., *Porosira* sp. and *Achyla* sp. (OTU E4-57 and phylotypes E4-124, E1-151 and E1-38). Pennate diatoms were represented by sequences related to *Fragilariopsis* sp., *Navicula* sp. and *Fragilaria* sp. The OTUs E1-43 and E1-160 were most related to sequences of the pennate diatoms *Nitzschia* sp. and *Haslea* sp. The phylotype E4-04 was related to *Paraphysomonas imperforata; Chrysophyceae*, a member of the Stramenopiles. The E4-01 phylotype appeared to represent a yet uncultivated OTU with 87% and 95% sequence similarity to *Bicosoeca* sp. (Stramenopile) and environmental clone UEPAC0p5, respectively.

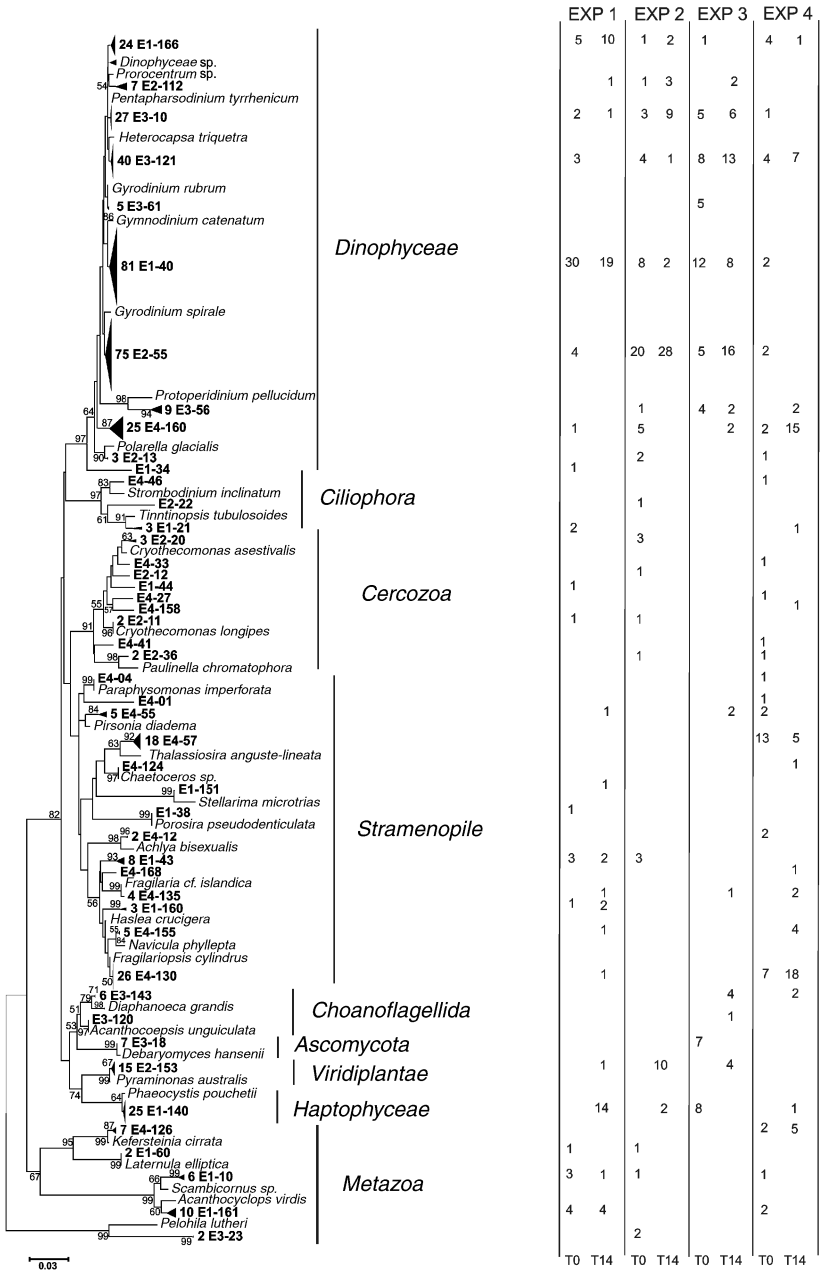

Fig. 4. Neighbor-joining phylogenetic tree of partial 18S rRNA gene sequences obtained from clones of T_0 and $T_{14(P)}$ from all experiments. For clarity purposes, clone sequences with at least 97% identity were clustered within OTUs. The number of clones held within each OTU is indicated at the front of the OTU name. On the right hand side, the clones are distributed per OTU for the 10 μm fraction of each experiment at T_0 and T_{14}. Note that the codes mentioned express experiment number and sequence number derived from DGGE. E3 stands for experiment 3; sequence numbers < 100 represent clones from T_0 samples; sequence numbers > 100 are derived from T_{14} samples. For example E3-126, is clone 26 taken at T_{14} from experiment 3.

The *Haptophyceae* were represented by 25 clones closely related to *Phaeocystis pouchetii*, which formed the OTU E1-140. A single OTU (E2-153) consisting of 15 clones represented the *Viridiplantae*, also called Chloroplastida (Adl *et al*., 2005), and were closely related to *Pyramimonas* sp. Two OTUs were closely related to the *Choanoflagellida*: six sequences clustered within OTU E3-143 closely related to *Diaphanoeca grandis* and the phylotype E3-120 related to *Acanthocoepsis* sp. E3-18 OTU (seven clones) was related to the yeast *Debaryomyces hansenii* (*Ascomycota*). Twelve clones belonged to the Cercozoa division; these included three OTUs (E4-33, E2-11 and E2-36) and five phylotypes. All cercozoan clones showed most similarity to sequences from *Cryothecomonas aestivalis* and *Cryothecomonas longipes* (*Cercozoa*), except OTU E2-36 which was most similar to *Paulinella chromatophora* (93%) and represents a yet uncultivated OTU.

Within the sequenced clones, it appeared that 27 belonged to the Metazoa. The sequences were divided into five OTUs: E1-60 (*Mollusca*), E4-126 (*Annelida*), E3-23 (*Platyhelminthes*), E1-10 and E1-161, both related to the Copepoda. The *Platyhelminthes* OTU E3-23 was novel, with 93% similarity to *Pelophila luteri* sequences.

Relative eukaryotic community diversity

The relative eukaryotic diversity of the sequenced samples was expressed in number of clones per OTU (Fig. 4), showing that dinoflagellates were abundant in all experiments. This is in agreement with microscopy data (P.G. Thomson, pers. commun.) and the DGGE analysis, where several bands present throughout the experiments proved to be related to dinoflagellates. Keeping in mind that DNA extraction, PCR amplification and cloning steps in combination with the limited number of sequenced clones may have induced biases in the generated dataset, the relative clone abundances described in the following paragraph only indicate trends in the clone abundances but do not give an exact quantitative measure of the extant community biodiversity.

In experiment 1, 75% of the inoculum community consisted of Alveolates, most of which were closely related to the *Dinophyceae*. Several Metazoan clones were also present. Sequences generated from the PAR sample after 14 days of incubation were still dominated by *Dinophyceae*-related sequences (54%), whereas the relative abundance of clones related to *Phaeocystis* sp. (23%) and Stramenopiles increased. In the second and third experiment, clones related to the *Dinophyceae* also dominated. This relative dominance of dinoflagellates persisted up to 14 days of incubation, although *Pyramimonas* sp. and a few *Phaeocystis* sp.-related sequences appeared. In experiments 2 and 3, *Pyramimonas* sp.-related sequences were detected after 14 days of incubation, whereas the relatively abundant *Phaeocystis* sp.-related sequences disappeared during experiment 3. In the Stramenopile-dominated community of experiment 4, sequences related to centric diatoms initially dominated the clone library. This group was replaced by pennate diatom-related sequences after 14 days of incubation. *Dinophyceae*-related sequences were still abundant, and yet the dominant OTU E4-160 differed from the other experiments. Overall experiments 2 and 3 communities were highly similar based on shared OTUs and clone abundances, while experiments 1 and 4 harbored distinct eukaryotic communities.

Discussion

Effects of solar irradiance on community composition

We used DGGE analysis of 18S rRNA gene fragments and partial-length 18S rRNA gene sequence analysis to gain an insight into the community structure of eukaryotic marine microorganisms in the Antarctic coastal sea in response to incident UV irradiation. The application of DGGE to assess shifts in prokaryotic and eukaryotic community composition after varying incubation periods has been used in numerous studies (Schäfer *et al.*, 2000, 2001; Massana *et al.*, 2001; Casamayor *et al.*, 2002; Vázquez-Domínguez *et al.*, 2005). Winter *et al.* (2001) successfully used DGGE to determine shifts in North Sea bacterioplankton communities after exposure to distinct irradiance regimes. In that study, small but consistent shifts in the DGGE patterns were revealed after exposure to UV-B and to a lesser extent UV-A radiation (315–400 nm).

Microscopy examination during the minicosm experiments revealed occasional subtle shifts in the relative abundances of several species (P.G. Thomson, unpublished results); this could not be confirmed by our data as DGGE is not a quantitative tool. The DGGE data did indicate occasional shifts in accordance with highest UV irradiance; however, statistical analysis of the environmental variables revealed that UV-R did not explain the variation in our data, which was only significantly explained by time and fraction size variable. Apparently, time and size-fraction were such strong factors in shaping the communities that they might overshadow a putative effect of UV dose. Although DGGE is clearly capable of revealing community shifts, it may lack the resolution to detect subtle shifts induced by weaker factors, such as UVR. Previous studies have demonstrated UV-B-related shifts in community composition, but used different experimental conditions, different starting communities and different means of assessing community composition. In previous studies, communities were generally incubated for 7 days, in volumes varying from 40 to 1500 L, under natural solar UV-R and, in some cases, under artificially enhanced UV-B radiation (Villafañe *et al.*, 1995; Mousseau *et al.*, 2000; Davidson & Belbin, 2002; Wängberg & Wulff, 2004). Shifts in species composition were generally assessed by microscopy, while supplementary pigment analysis provided quantitative data on major phytoplankton groups. In several of those studies, dinoflagellates appeared to be less affected by UVB than diatoms (Mousseau *et al.*, 2000; Davidson & Belbin, 2002). In contrast, incubations of Antarctic communities under UV-R by Villafañe *et al.* (1995) lead to a relative increase in diatoms at the expense of nanoflagellates. Experiments conducted in the St Lawrence Estuary by Mostajir *et al.* (1999) showed that natural UV-B did not affect community composition. Instead, community composition and the pelagic food-web structure were only affected when UV-B irradiance was artificially increased. Similar to our findings their conclusion was that natural UV-R regimes do not trigger significant shifts in the major eukaryote groups.

Effects of incubation on community diversity

Countway *et al.* (2005) incubated natural sea-water samples under ambient irradiance and temperatures for 72 h. Molecular analyses on partial length 18S rRNA gene carried out by terminal restriction fragment length polymorphism (t-RFLP) revealed minor changes in the microbial eukaryotic

richness. Shifts in community composition and dominant eukaryotic species were observed over time. Similar observations using identical molecular methods were made for natural marine bacterial assemblages (Schäfer *et al.*, 2000; Massana *et al.*, 2001; Massana & Jürgens, 2003) and natural marine protistan assemblages (Massana & Jürgens, 2003) incubated under varying conditions and periods. In our minicosm experiments, shifts in the microeukaryotic community composition and in dominant eukaryotic species were observed after 7 and 14 days of incubation (Figs 2 and 4). However, the diversity indices calculated from our data were variable (Table 3). Sequencing data revealed a stable diversity in experiments 1 ($H' = 2.02$) and 3 ($H' = 2.10$) and a decreased diversity during incubation in experiment 2 ($H'_0 = 2.34$ to $H'_{14} = 1.53$) and experiment 4 ($H'_0 = 2.65$ to $H'_{14} = 2.19$). The DGGE data also indicated variable diversity indices. In experiments 1 and 3, DGGE data (number of bands) revealed an increase in diversity. Diversity calculated for DGGE data from experiment 2 remained stable over time, whereas diversity decreased in experiment 4. Diversity calculated from sequencing and DGGE data generally diverged, except for the decrease in diversity from experiment 4. The experiments suggest that incubating light limited subsea-ice marine eukaryotic communities (communities from experiments 1, 2 and 3) into tanks replenished in light leads to an increase in diversity, suggesting that the incubation conditions provided in the minicosms favored the growth of a new community of species. Marine microeukaryotes collected after sea-ice break up, communities from experiment 4, had a higher initial diversity ($H'_0 = 2.65$), suggesting that the exposure to more light, due to the sea ice disappearance, already induced the growth of a new community of microeukaryote species. Incubating this community caused a shift towards a few dominant species as indicated by the reduced diversity, OTU and band numbers.

Community composition

Three different communities emerged from our experiments. The first community was composed of dinoflagellates, ciliates, diatoms, *Phaeocystis* sp., *Pyramimonas* sp. and several metazoan species, including copepods. This community persisted throughout experiment 1 and was derived from a postwinter seed population, which can harbor relatively large numbers of *Phaeocystis* sp. cells. This is supported by several Antarctic field surveys: Davidson & Marchant (1992) observed an early *P. pouchetii* spring bloom in Prydz Bay; others made similar observations in the Ross Sea (El-Sayed *et al.*, 1983; DiTullio *et al.*, 2000). Most metazoan sequences found in experiment 1 were derived from sympagic (ice associated) grazers often located under the ice where they graze on ice algae (Karl, 1993; Le Fèvre *et al.*, 1998).

The second community, mainly comprising samples from experiments 2 and 3, was largely dominated by dinoflagellates, whereas diatoms were insignificant as confirmed by microscopy (P.G. Thomson, pers. commun.). In a dinoflagellate-dominated community, autotrophic, heterotrophic and mixotrophic dinoflagellates can coexist. Some of the OTUs defined in the phylogenetic tree (Fig. 4) such as *Gyrodinium* sp. are heterotrophic. For example, a few *Gyrodinium* species, including *Gyrodinium spirale*, *Gyrodinium fusiforme* and *Gyrodinium dominance*, were successfully cultivated when fed with nanoflagellates, Raphidophytes, dinoflagellates or diatom preys (reviewed in Tillman, 2004). Several studies using molecular tools to determine the microeukaryotic community composition have observed a high diversity for dinoflagellates (López-Garciá *et al.*, 2001; Moreira & Lopez-Garcia, 2002; Moon-van der Saay *et al.*, 2003). Our data confirm that Antarctic coastal sites harbor numerous dinoflagellates species. Previous studies on fast ice communities have shown an increase of ice brine dinoflagellate, s.a. *Polarella glacialis*, in the water column during late spring sea ice melting periods (Kivi & Kuosa, 1994; Thomson *et al.*, 2006). Samples from experiments 2 and 3 were collected in December 2002 at the onset of sea ice melting; this might have contributed to the dinoflagellate dominance. The third, diatom-dominated community appeared in the final experiment that was conducted in January. The diatom dominance was indicated by our sequencing data and confirmed by microscopy.

Overall, our T_0 samples provided an insight into the marine microbial eukaryotic communities developing from November 2002 to January 2003 in Prydz Bay. However, the community composition of the tanks after 14 days of

Table 3. Sequence and DGGE data diversity indices from communities exposed to PAR irradiance

	Experiment 1			Experiment 2			Experiment 3			Experiment 4				
	T_0	T_7	T_{14}	T_0	T_7	T_{14}	T_0	T_7	T_{14}	T_0	T_7	T_{14}	Average	SD
OTUs	16	ND	15	18	ND	8	9	ND	12	21	ND	15		
H'*	2.02	ND	2.02	2.34	ND	1.53	2.07	ND	2.12	2.65	ND	2.19	2.12	0.32
Bands	9	16	13	17	17	17	12	18	21	18	19	10		
H'†	1.90	2.44	2.19	2.58	2.62	2.41	2.16	2.57	2.54	2.65	2.51	1.69	2.26‡	0.34

H' Shannon–Wiener diversity index was calculated for *sequence data, †DGGE data of T_0, $T_{7(P)}$ and $T_{14(P)}$ samples, and ‡average for T_0 and T_{14} DGGE data.

incubation did not correspond to the inoculum of the following experiment, indicating that the communities incubated in the tanks developed differently than in Prydz Bay. Typically, postwinter Antarctic water is replete in nutrients and silicic acid, such that as soon as light limitation is eliminated a diatom bloom is triggered (Bidle & Azam, 1999). In our experimental setup, incubation of the sub ice community in the light did not induce a diatom bloom, suggesting that advective processes or melting sea-ice need to be invoked to explain the supply of the initial seed population for the initiation of a diatom bloom.

Antarctic eukaryotic diversity and species composition

Most studies conducted on the Antarctic protozoan diversity have been performed in the Marginal Ice Zone and at the Polar Front. Therefore, data on Antarctic coastal sites remain scarce and are generally limited to microscopy. Based on these data, coastal Antarctic systems were long considered to harbor low microeukaryotic diversity (Karl, 1993). However, our molecular data revealed a diversity averaging 2.12 and 2.26 (Shannon–Wiener index, shown in Table 3). The highest diversity calculated for natural samples (inocula) in our data set was 2.65 obtained from sequence and DGGE data of samples from experiment 4; the lowest diversity was 2.02 and 1.90 for sequencing and DGGE data, respectively. As a comparison, microscopy data on the diversity of the microeukaryotic community gathered for another Antarctic coastal site directly under the ice in late spring 1995, revealed a diversity of 0.67 and 1.87 (Riaux-Gobin *et al*., 2003). Molecular (DGGE) and microscopy analysis of surface seawater samples collected in the Bay of Fundy, Western North Atlantic, showed phytoplankton diversities varying from 1.16 to 2.55 throughout summer (Savin *et al*., 2004). Countway *et al*. (2005) also analyzed protistan diversity from the Western North Atlantic, by applying another PCR-based community fingerprinting technique t-RFLP and found diversities (Shannon–Wiener index) in the range of 0.99–1.44. Only a few studies have published data on marine microeukaryotic diversity, often applying different molecular methods, each with a varying resolution level. Keeping resolution differences in mind, our data suggest that the microeukaryotic community from Prydz Bay in spring/summer 2002 had a similar, but slightly higher diversity as compared with other diversity studies.

Dinoflagellates largely dominated our inocula samples, which provided a representation of the Prydz Bay community from November 2002 to January 2003. In experiments 2 and 3, dinoflagellates were represented by 10 distinct OTUs, of which only two showed low similarities to any known sequences ($< 93\%$). One of these, the OTU E4-160 mainly found in experiment 4, was represented by 25 clones. A recent study in the Antarctic region, reporting a novel dinoflagellate (Gast *et al*., 2006), suggests that several dinoflagellates from Antarctic waters have yet to be described, or are possibly missed during classical microscopy analysis due to their ambiguous morphological features. Their dominance underlines the essential role of dinoflagellates in the coastal Antarctic system in the postwinter/early spring period and in between bloom events.

The Stramenopiles were represented by centric and pennate diatoms, principally *Thalassiosira* sp. and *Fragilariopsis* sp. Among the Stramenopiles, OTU E4-55 and phylotypes E4-01 represented uncultivated strains. According to the MAST (Marine Stramenopile) classification proposed by Massana *et al*. (2004) OTU; E4-55 belongs to the MAST 1 group and is closely related to their ME1-21 clone. OTU E4-12 showed 95% similarity to *Achyla bisexualis*, an Oomycetes, a member of the Stramenopiles. The phylotype E4-01 distantly clustered with a MAST 3 clone (HE427-21), but with only 94% similarity (Massana *et al*., 2004).

The 18S rRNA gene clone library contained representatives of the heterotrophic Choanoflagellates (*Diaphanoeca* sp. and *Acanthocoepsis* sp.) (Thomsen *et al*., 1990; Leaky *et al*., 2002). Here, the choanoflagellida OTU E3-143 was the closest to *Diaphoneaca grandis* sequence (Accession AF084234). Using microscopy, *Parvicorbicula socialis* was identified as the most dominant choanoflagellate species present (P.G. Thomson, unpublished results). *Parvicorbicula socialis* 18S rRNA gene has not yet been sequenced. At the same time, no *Diaphoneaca grandis* cells were detected using microscopy. It is, therefore, likely that the Choanoflagellate OTU E3-143 represents *Parvicorbicula* sp.

Cryothecomonas sp. and several novel phylotypes (E4-33, E2-12, E1-44, E4-158 and E4-27) were closely related in the phylogenetic tree. *Cryothecomonas* sp. has two described strains: *Cryothecomonas aestivalis* and *Cryothecomonas longipes*, relatives were both most related to sequences found in our experiments. Small subunit (18S rRNA gene) sequencing results have suggested that they belong to the *Cercozoa* (Kuhn *et al*., 2000; Bass & Cavalier-Smith, 2004). Here, we add four novel phylotypes to this group, some of which clustered best with uncultured cercozoan clones from the Arctic (Lovejoy *et al*., 2006) and all clustered in between the *C. longipes* and *C. aestivals*. Two additional novel phylotypes were closely related to *Paulinella chromatophora*, which belongs to the *Eugliphyta* order of the cercozoans (Cavalier-Smith & Chao, 2003).

In this study, we recovered a sequence very similar to the halotolerant yeast, *D. hansenii* (E3-18). This organism has been found previously in natural salterns, cold sea-water habitats and also in Antarctic permafrost cryopegs (Butinar *et al*., 2005; Gilinchinski *et al*., 2005). Microscopy confirmed the presence of strands of coccoid yeast cells. Although we cannot fully exclude the possibility of contamination during

sampling, our data suggest that this yeast species might also be present in marine Antarctic waters. It is, however, unknown whether they are part of an active population.

Conclusion

Incubation of natural coastal Antarctic $< 200\,\mu m$ communities under distinct UV-R irradiation regimes induced sporadic shifts in the community structure, however, the influence of UV-R on the community structure was not significant. Changes in DGGE band patterns were mainly found according to incubation time and fraction size; both variables explained a significant part of our DGGE data set. Sequencing data on the composition of the inocula revealed that dinoflagellates dominated Prydz Bay microeukaryotic community from November to December 2002. In January 2003, when sea ice broke up, a diatom bloom was initiated that was superimposed on the assemblages found earlier. Application of molecular analytical tools revealed a moderate diversity and provided an insight into the Antarctic coastal dinoflagellate species composition that would otherwise be underestimated when applying microscopy only due to cryptic taxonomic features. Among the 11 dinophycean phylotypes, two were novel dinoflagellate strains and one yet uncultivated dinoflagellate strain, with $< 93\%$ sequence similarity to any cultivated dinoflagellate strain. Moreover, one novel ciliate strain, one novel metazoan OTU, one uncultivated cercozoan strain and one uncultivated Stramenopile strain were detected. The present study underlines the relevance of applying molecular techniques for future marine polar diversity studies. Applying a combination of molecular methods and classical microscopy analysis with increasing cultivation efforts may delineate the large collection of 'unknown' sequences and reveal their function in the ecosystem.

Acknowledgements

We are grateful for the sequencing work performed by Ing. J.K. Brons. We would like to thank the Davis Station personnel for the good support during the field campaign. Also, we are grateful for the sample filtering support provided by Marjolein van Polanen-Petel, Tamara van Polanen-Petel and Paul Janknegt. We thank three anonymous reviewers for their valuable comments that greatly improved the quality of the manuscript. This research was financed by the Australian Antarctic Division and NWO.

References

Adl SM, Simpson AG, Farmer MA *et al.* (2005) The new higher level classification of eukaryotes with the emphasis on the taxonomy of protists. *J Euk Microb* **52**: 399–451.

Arrigo KR, Robinson DH, Worthern DL, Dunbar RB, DiTullio GR, VanWoert M & Lizotte MP (1999) Phytoplankton community structure and the drawdown of nutrients and CO_2 in the Southern Ocean. *Science* **283**: 365–367.

Arrigo KR, Lubin D, van Dijken GL, Holm-Hansen O & Morrow E (2003) Impact of a deep ozone hole on Southern Ocean primary production. *J Geophys Res* **108**: 1–19.

Bass D & Cavalier-Smith T (2004) Phylum-specific environmental DNA analysis reveals remarkably high global biodiversity of *Cercazoa* (Protozoa). *Int J Syst Evol Microbiol* **54**: 2393–2404.

Bidle KD & Azam F (1999) Accelerated dissolution of diatom silica by marine bacterial assemblages. *Nature* **397**: 508–512.

Buma AGJ, Boer dMK & Boelen P (2001) Depth distribution of DNA damage in Antarctic marine phyto- and bacterioplankton exposed to summertime UV radiation. *J Phycol* **37**: 200–208.

Butinar L, Santos S, Spencer-Martins I, Oren A & Gunde-Cimerman N (2005) Yeast diversity in hypersaline habitats. *FEMS Microbiol Lett* **244**: 229–234.

Casamayor EO, Massana R, Benlloch S, Øvreås L, Díez B, Goddard VJ, Gasol JM, Joint I, Rodríguez-Valera F & Pedrós-Alió C (2002) Changes in archeal, bacterial and eukaryal assemblages along a salinity gradient by comparison of genetic fingerprinting methods in a multipond solar saltern. *Environ Microbiol* **4**: 338–348.

Cavalier-Smith T & Chao EE-Y (2003) Phylogeny and classification of phylum *Cercazoa* (Protozoa). *Protist* **154**: 341–358.

Countway PD, Gast RJ, Savai P & Caron DA (2005) Protistan diversity estimates based on 18S rDNA from seawater incubations in the Western North Atlantic. *J Euk Microb* **52**: 95–106.

Davidson AT & Belbin L (2002) Exposure of natural Antarctic marine microbial assemblages to ambient UV radiation: effects on the marine microbial community. *Aquat Microb Ecol* **27**: 159–174.

Davidson AT & Marchant HJ (1992) Protist abundance and carbon concentration during a *Phaeocystis*-dominated bloom at an Antarctic coastal site. *Pol Biol* **12**: 387–395.

Davidson AT, Bramich D, Marchant HJ & McMinn A (1994) Effects of UV-B irradiation on growth and survival of Antarctic marine diatoms. *Mar Biol* **119**: 507–515.

Díez B, Pedrós-Alió C, Marsh TL & Massana R (2001) Application of denaturing gradient gel electrophoresis (DGGE) to study the diversity of marine picoeukaryotic assemblages and comparison of DGGE with other molecular techniques. *App Env Microbiol* **67**: 2942–2951.

DiTullio GR, Grebmeier JM, Arrigo KR, Lizotte MP, Robinson DH, Leventer A, Barry JP, van Woert ML & Dunbar RB (2000) Rapid and early export of *Phaeocystis antarctica* blooms in the Ross Sea, Antarctica. *Nature* **404**: 595–598.

DiTullio GR, Geesey ME, Jones DR, Daly KL, Campbell L & Smith WO Jr (2003) Phytoplankton assemblage structure and

primary productivity along 170°W in the Southern Pacific Ocean. *Mar Ecol Prog Ser* **255**: 55–80.

El-Sayed SZ (1993) Phytoplankton. *Antarctic Microbiology* (Friedman EI & Thistle AB, eds), pp. 67–122. Wiley-Liss, New York.

El-Sayed SZ, Biggs DC & Holm-Hansen O (1983) Phytoplankton standing crop, primary productivity, and near-surface nitrogenous nutrient fields in the Ross Sea, Antarctica. *Deep Sea Res Part A Oceanogr Res Pap* **30**: 871–886.

Falkowski PG, Barber RT & Smetacek V (1998) Biogeochemical controls and feedbacks on ocean primary production. *Science* **281**: 200–206.

Felsenstein J (1985) Confidence limits on phylogenies: an approach using the bootstrap. *Evolution* **39**: 783–791.

Gast RJ, Dennett MR & Caron DA (2004) Characterization of protistan assemblages in the Ross Sea, Antarctica, by denaturing gradient gel electrophoresis. *App Environ Microbiol* **70**: 2028–2037.

Gast RJ, Moran DM, Beaudoin DJ, Blythe JN, Dennett MR & Caron DA (2006) Abundance of a novel dinoflagellate phylotype in the Ross Sea, Antarctica. *J Phycol* **42**: 233–242.

Gilinchinski D, Rivkina E, Bakermans C *et al.* (2005) Biodiversity of cryopegs in permafrost. *FEMS Microbiol Ecol* **53**: 117–128.

Hartl DL, Moriyama EN & Sawyer SA (1994) Selection intensity for codon bias. *Genetics* **138**: 227–234.

Holm-Hansen O, Helbling EW & Lubin D (1993) Ultraviolet radiation in Antarctica: inhibition of primary production. *Photochem Photobiol* **58**: 567–570.

Huntley ME, Lopez MD & Karl DM (1991) Top predators in the Southern Ocean: a major leak in the biological pump. *Science* **253**: 64–66.

Karentz D, Cleaver JE & Mitchell DL (1991) Cell survival characteristics and molecular responses of Antarctic phytoplankton to ultraviolet-B radiation. *J Phycol* **27**: 326–341.

Karl DM (1993) Microbial processes in the Southern Ocean. *Antarctic Microbiology* (Friedmann EI & Thistle AB, eds), pp. 1–63. Wiley-Liss, New York.

Kimura MJ (1980) A simple method of estimating evolutionary rates of base substitutions through comparative studies of nucleotide sequences. *J Mol Evol* **16**: 150–163.

Kivi K & Kuosa H (1994) Late winter microbial communities in the western Wedell Sea. *Pol Biol* **14**: 389–399.

Kuhn S, Lange M & Medlin LK (2000) Phylogenetic position of *Cryothecomonas* inferred from nuclear-encoded small subunit ribosomal RNA. *Protist* **151**: 337–345.

Kumar S, Tamura K & Nei M (2004) MEGA3: integrated software for molecular evolutionary genetics analysis and sequence alignment. *Brief Bioinform* **5**: 150–163.

Leaky RJG, Leadbeater BSC, Mitchell E, McCready SMM & Murray AWA (2002) The abundance and biomass of choanoflagellates and other nanoflagellates in waters of contrasting temperature to north-west of South-Georgia in the Southern Ocean. *Eur J Protist* **38**: 333–350.

Le Fèvre J, Legendre L & Rivkin RB (1998) Fluxes of biogenic carbon in the Southern Ocean: roles of large microphagous zooplankton. *J Mar Syst* **17**: 325–345.

López-Garciá P, Rodríguez-Valera F, Pedrós-Alió C & Moreira D (2001) Unexpected diversity of small eukaryotes in deep sea Antarctic plankton. *Nature* **409**: 603–607.

Lovejoy C, Massana R & Pedrós-Alió C (2006) Diversity and distribution of marine microbial eukaryotes in the Arctic Ocean and adjacent seas. *App Environ Microbiol* **72**: 3085–3095.

Massana R & Jürgens K (2003) Composition and population dynamics of planktonic bacteria and bacteriovorous flagellates in seawater chemostat cultures. *Aquat Microb Ecol* **32**: 11–22.

Massana R, Pedrós-Alió C, Casamayor EO & Gasol JP (2001) Changes in marine bacterioplankton phylogenetic composition during incubations designed to measure biogeochemically significant parameters. *Limnol Oceanogr* **46**: 1181–1188.

Massana R, Castresana J, Balagué V, Guillou L, Romari K, Groisiller A, Valentin K & Pedrós-Alió C (2004) Phylogenetic and ecological analysis of novel marine Stramenopiles. *App Environ Microbiol* **70**: 3528–3534.

Medlin LK, Elwood HJ, Stikel S & Sogin M (1988) The characterization of enzymatically amplified eukaryotic 16S-like rRNA-coding regions. *Gene* **71**: 491–499.

Moon-van der Saay SY, Wachter De R & Vaulot D (2003) Oceanic 18S rDNA sequences from picoplankton reveal unsuspected eukaryotic diversity. *Nature* **409**: 607–610.

Moreira D & Lopez-Garcia P (2002) The molecular ecology of microbial eukaryotes unveils a hidden world. *Trends Microbiol* **10**: 31–38.

Mostajir B, Demers S, Mora Sd, Belzile C, Chanut J-P, Gosselin M, Roy S, Zulema Villegas P, Fauchot J & Bouchard J (1999) Experimental test of the effect of ultraviolet-B radiation in a planktonic community. *Limnol Oceanogr* **44**: 586–596.

Mousseau L, Gosselin M, Levasseur M, Demers S, Fauchot J, Roy S, Villeags PZ & Mostajir B (2000) Effects of ultraviolet-B radiation on simultaneous carbon and nitrogen transport rates by estuarine phytoplankton during a week-long mesocosm study. *Mar Ecol Prog Ser* **199**: 69–81.

Muyzer G, Brinkhoff T, Nübel U, Santegoeds C, Schäfer H & Wawer C (2004) Denaturing gradient gel electrophoresis (DGGE) in microbial ecology. *Molecular Microbial Ecology Manual* (Kowalchuk GA, de Bruin FJ, Head IM, Akkermans DL & van Elsas JD, eds), pp. 743–770. Kluwer Academic Publishers, Dordrecht.

Raven JA & Falkowski PG (1999) Oceanic sinks for atmospheric CO_2. *Plant Cell Environ* **22**: 741–755.

Riaux-Gobin C, Poulin M, Prodon R & Treguer P (2003) Land-fast ice microalgal and phytoplanktonic communities (Adélie Land, Antarctica) in relation to environmental factors during ice break-up. *Antarc Sci* **15**: 353–364.

Saitou N & Nei M (1987) The neighbor-joining method: a new method for reconstructing phylogenetic trees. *Mol Biol Evol* **4**: 406–425.

Savin MC, Martin JL, LeGresley M & Rooney-Varga J (2004) Plankton diversity in the Bay of Fundy as measured by morphological and molecular methods. *Microb Ecol* **48**: 51–63.

Sambrook J, Fritsch EF & Maniatis T (1989) *Molecular Cloning: A Laboratory Manual*. Cold Spring Harbor Laboratory Press, Cold Spring Harbor, New York.

Schäfer H, Servais P & Muyzer G (2000) Successional changes in the genetic diversity of a marine bacterial assemblage during confinement. *Arch Microbiol* **173**: 138–145.

Schäfer H, Bernard L, Courties C, Lebaron P, Servais P, Pukall R, Vives-Rego J & Muyzer G (2001) Microbial community dynamics in Mediterranean nutrient-enriched seawater mesocosms: changes in genetic diversity of bacterial populations. *FEMS Microbiol Ecol* **34**: 243–253.

Shepherd A & Wingham D (2007) Rescent sea-level contributions of the Antarctic and Greenland ice sheet. *Science* **315**: 1529–1532.

Tamura K, Dudley J, Nei M & Kumar S (2007) MEGA4: molecular evolutionary genetics analysis (MEGA) software version 4.0. *Mol Biol Evol* **24**: 1596–1599.

ter Braak CJF & Šmilauer P (1998) *CANOCO Reference Manual and User's Guide to Canoco for Windows: Software for Canonical Community Ordination (Version 4.5.2)*. Microcomputer Power Ed., Ithaca, New York.

Thomsen HA, Bucks KR, Coale SL, Garrison DL & Gowing MM (1990) Loricate choanoflagellates (Acanthoecidea, Choanoflagellida) from the Wedell Sea, Antarctica. *Zool Scr* **19**: 367–287.

Thomson PG, McMinn A, Kiessling I, Watson M & Goldsworthy PM (2006) Composition and succession of dinoflagellates and chrysophytes in the upper fast ice of Davis Station, Eastern Antarctica. *Pol Biol* **29**: 337–345.

Tillman U (2004) Interactions between plankton microalgae and protozoan grazers. *J Euk Microb* **52**: 156–168.

Vázquez-Domínguez E, Casamayor EO, Català P & Lebaron P (2005) Different marine heterotrophic nanoflagellates affect differentially the composition of enriched bacterial communities. *Microb Ecol* **49**: 474–485.

Villafañe VE, Helbling EW, Holm-Hansen O & Chalker BE (1995) Acclimatization of Antarctic natural phytoplankton assemblages when exposed to solar ultraviolet radiation. *J Plankton Res* **17**: 2295–2306.

Wängberg S-Å & Wulff A (2004) Impact of UVB radiation on the development of phytoplankton communities in the eastern Atlantic sector of the Southern Ocean – results from an on-deck model ecosystem experiments. *Deep Sea Res Part II Oceanogr Res Pap* **51**: 2731–2744.

Weber LH & El-Sayed SZ (1987) Contributions of the net, nano- and picoplankton to the phytoplankton standing crop and primary productivity in the Southern Ocean. *J Plankton Res* **9**: 973–994.

Winter C, Moeseneder MM & Herndl GJ (2001) Impact of UV radiation on bacterioplankton community composition. *App Environ Microbiol* **67**: 665–672.

Zhu L & Bustamante CD (2005) A composite-likelihood method for detecting directional selection from DNA sequence data. *Genetics* **170**: 1411–1421.